

**This is the preprint version of the contribution published as:**

Dalby, F.R., Hansen, M.J., Feilberg, A., **Kümmel, S., Nikolausz, M.** (2020):  
Effect of tannic acid combined with fluoride and lignosulfonic acid on anaerobic digestion in  
the agricultural waste management chain  
*Bioresour. Technol.* **307** , art. 123171

**The publisher's version is available at:**

<http://dx.doi.org/10.1016/j.biortech.2020.123171>

1 Title

2 Effect of tannic acid combined with fluoride and lignosulfonic acid on anaerobic  
3 digestion in the agricultural waste management chain.

4 Author names

5 Frederik R. Dalby<sub>1</sub>, Michael J. Hansen<sub>1</sub>, Anders Feilberg<sub>1</sub>, Steffen Kümmel<sub>2</sub>, Marcell  
6 Nikolausz<sub>3</sub>\*

7 Affiliation

8 <sub>1</sub>Department of Engineering, Air Quality Engineering, Aarhus University, 8200 Aarhus  
9 C, Denmark. <sub>2</sub>Department of Isotope Biogeochemistry, Helmholtz Centre for  
10 Environmental Research-UFZ, 04318 Leipzig, Germany, <sub>3</sub>Department of  
11 Environmental Microbiology, Helmholtz Centre for Environmental Research-UFZ,  
12 04318 Leipzig, Germany

\*Corresponding Author.

E-mail address: marcell.nikolausz@ufz.de (M. Nikolausz).

## 13 Abstract

14 Livestock waste is stored and used as soil fertilizer or directly as substrate for biogas  
15 production. Methane emissions from manure storages and ammonia inhibition of  
16 anaerobic digesters fed with manure, are well-known problems related to manure  
17 management. This study examines the effect of adding tannic acid with fluoride (TA-  
18 NaF) and lignosulfonic acid (LS) on methanogenic activity in batch reactors with  
19 ammonia inhibited maize silage digestate and in batch reactors with manure.  
20 Lignosulfonic acid counteracted urea induced ammonia inhibition of methanogenesis,  
21 whereas TA-NaF inhibited methanogenesis itself. Stable carbon isotope ratio analysis  
22 and methanogen community analysis suggested that TA-NaF affected acetoclastic  
23 methanogens the most. The combined findings suggest that TA-NaF could be used to  
24 reduce methane emissions from stored manure. Conversely, LS could be used as  
25 supplement in anaerobic digesters prone to urea induced ammonia inhibition.

## 26 Keywords

27 Anaerobic digestion, Ammonia inhibition, Stable isotope, Methanogens, Tannic acid

## 28 1. Introduction

29 Agricultural waste holds a vast potential as nutrient and energy source if managed  
30 properly (Westerman and Bicudo, 2005), whereas improper management may result in  
31 increased environmental pollution and greenhouse gas emissions (Holly et al., 2017).  
32 Anaerobic digestion (AD) may extract value from agricultural waste by producing  
33 biogas, which fuels heat or power generation at combined heat and power units (Wu et  
34 al., 2016). The digestate from AD maintains its value as a fertilizer, and it has been  
35 suggested to emit less odorants upon subsequent landspreading (Hansen et al., 2006).  
36 Under some circumstances, the waste is not used for AD owing to challenges with  
37 manure transport to an AD facility, national regulations or AD inhibiting constituents  
38 such as ammonia. Ammonia in AD arises mainly from dietary protein catabolism and  
39 enzymatic urea hydrolysis by urease (Elzing and Monteny, 1997), and it exhibits an  
40 inhibitory effect on methanogenesis (Lv et al., 2019). Urease is produced in fecal  
41 material by ureolytic bacteria, and urea is excreted in urine (Elzing and Monteny, 1997).  
42 Consequently, manure fed AD frequently suffers from ammonia inhibition (Sun et al.,  
43 2016). In this scenario, composting or manure storage followed by landspreading is the  
44 conventional management route (Hou et al., 2015). However, manure storage and  
45 subsequent soil application is associated with methane emissions and significant N-loss  
46 in the form of ammonia or nitrous oxide, which reduce the fertilizer value and  
47 contribute to global warming (Lee et al., 2017; Sørensen and Amato, 2002).  
48 It is imperative that agricultural operations manage waste materials and reduce the  
49 environmental footprint in all parts of the waste management chain. In this regard,  
50 manure waste treatment with polyphenols may be a key strategy that can alter its  
51 applicability in AD or for storage and landspreading activities, thereby offering more

52 flexibility in the management chain. Polyphenols are a wide group of secondary plant  
53 metabolites containing large numbers of di and/or trihydroxyphenyl units (Bravo, 2009;  
54 Quideau et al., 2011), and have been identified as antimicrobial agents (Papuc et al.,  
55 2017). Tannic acid (TA) is a polyphenol consisting of gallic acid and polyol units  
56 (Bravo, 2009) that in combination with sodium fluoride (NaF) was found to mitigate  
57 ammonia, methane and volatile organic compounds emissions from manure (Dalby et  
58 al.)The mitigation of ammonia emissions was partially attributed to a synergism  
59 between TA and NaF that directly inhibited the urease enzyme, but it was also attributed  
60 to the inherent antimicrobial effects of TA, as claimed in other studies (Al-Jumaili et al.,  
61 2017; Whitehead et al., 2013). The urease inhibiting effect of TA could potentially be of  
62 value in ammonia inhibited AD. However, TA-NaF reduces methanogenic activity,  
63 obscuring the potential positive effect of urease inhibition. Therefore, TA-NaF may be  
64 more adequate as supplement to stored manure from which methane emissions should  
65 be abated. The pulp and paper industry byproduct, lignosulfonic acid (LS) (Calvo-  
66 Flores and Dobado, 2010), which contains similar functional hydroxyl groups to TA,  
67 may be an alternative supplement to urea rich AD substrates. Despite reported anti-  
68 methanogenic activity of some lignin derivatives, the inhibitory effect of these seems to  
69 be linked to low molecular weight lignins (Sierra-Alvarez, 2007).

70 The aim of this study was to elucidate the effect of TA-NaF and LS on methane  
71 production and methanogenic pathways in a standard biogas reactor (fed with inoculum  
72 from a maize silage fed reactor) and in stored swine manure, cattle manure, and poultry  
73 litter. Owing to the urease inhibiting activity of TA-NaF, it was hypothesized that LS  
74 would exhibit a similar urease inhibiting effect in urea loaded biogas reactor slurry and  
75 thereby increase the methane yield. Furthermore, it was hypothesized that TA-NaF may

76 inhibit acetoclastic methanogenesis, which would counteract the positive effect of  
77 urease inhibition in biogas reactors. The interpretation of methane yield, compound-  
78 specific stable isotope analysis of the produced biogas, and microbial community  
79 structure analysis were used to test these hypotheses. The findings hint to possible  
80 application areas of TA-NaF and LS in the manure management chain, which could  
81 advance the sustainability of agricultural activities.

82

## 83 2. Materials and methods

84 Figure 1 presents a schematic of the experimental work conducted in this study. The  
85 study consists of two parallel experiments in which digestate obtained from a biogas  
86 reactor fed with maize silage (hereinafter denoted as maize silage digestate) or different  
87 manure types were used as inocula. The maize silage digestate batch reactors were  
88 treated with TA-NaF, LS, urea, and/or cellulose as substrate, whereas manure reactors  
89 were treated with TA-NaF or LS. Besides the methods displayed in Figure 1, the  
90 inocula were also analyzed for relevant chemical characteristics.

91

### 92 2.1 Maize silage digestate batch reactor experiments

93 Two consecutive batch experiments were conducted using an automatic methane  
94 potential test system (AMPTS, Bioprocess control, Lund, Sweden) under mesophilic  
95 conditions (38 °C). Batch 1 and batch 2 was performed to test the effect of TA-NaF and  
96 LS under high urea load and without urea load, respectively. Table 1. compiles the  
97 reactor treatments of batch 1 and batch 2. As inoculum, degassed digestate from a large-  
98 scale biogas plant, operating with maize silage as a main substrate, was used (referred to  
99 as maize silage digestate). Each batch experiment lasted 30 days and included 15 x 500

100 mL reactors incubated with 350 g inoculum. The experiment was conducted under  
101 anaerobic conditions by initially flushing the reactors with nitrogen. Methane  
102 production was measured volumetrically, and carbon dioxide was removed by  
103 channeling the produced gas from the batch reactors through the headspace of a 100 mL  
104 3M sodium hydroxide solution with a thymolphthalein pH indicator prior to the  
105 volumetric gas detection unit according to the AMPTS default recommendations. The  
106 measured gas volumes were corrected to standard temperature (273.15 K) and pressure  
107 (101.32 kPa), then reported as normalized milliliters. A detailed description of the  
108 AMPTS setup is provided in the Supplementary materials. The reactors were  
109 supplemented with 1 % (w/w) cellulose (Sigma Aldrich CAS 9004-34-6) as substrate  
110 and 1% (w/w) urea-N (Sigma Aldrich, CAS 57-13-6) to induce ammonia inhibition. As  
111 a treatment, either 1% (w/w) liginosulfonic acid sodium salt (LS) (Sigma Aldrich, CAS  
112 8061-51-6) or 2.5 to 10 mM tannic acid (TA) (Sigma Aldrich, CAS 1401-55-4)  
113 combined with 1 mM sodium fluoride (NaF) (Sigma Aldrich, CAS 7681-49-4) was  
114 added. Demineralized water was added to level out volume differences between  
115 reactors. Each experimental treatment was performed in triplicates.

116 **2.1.1 Sampling and analyzes of maize silage digestate batch reactors.** The pH,  
117 volatile solids (VS), and total solids (TS) were measured at the beginning and end of the  
118 experiments. Samples for microbial community structure analysis, total ammonia  
119 nitrogen (TAN), and volatile fatty acids (VFA) analysis were collected at experiment  
120 start and end and stored at -18 °C until analysis. Gas samples for biogas composition  
121 and compound-specific isotope analysis were collected every 2-4 day through a  
122 customized gas sampling port with rubber septa inserted in TYGON tubings between

123 the reactors and the CO<sub>2</sub> trap of the AMPTS. The gas samples were stored in 20 mL  
124 argon flushed vials until analysis.

125

## 126 2.2 Manure batch reactor experiments

127 Swine manure (2% VS), cattle manure (7.5% VS), and poultry litter (50% VS) was  
128 initially diluted to the same VS content (2%) with demineralized water. Then 36 x 200  
129 mL serum bottles were each inoculated with 120 g of the diluted manure without  
130 additional cellulose substrate. The reactor headspaces were flushed with nitrogen to  
131 obtain an anaerobic environment. Eighteen of the reactors were incubated at room  
132 temperature (~23 °C) and 18 reactors were incubated at 38 °C using a heating chamber.  
133 Incubation at room temperature simulated manure storage conditions, whereas  
134 incubation at 38 °C was prepared to enhance methanogenic activity and simulate a  
135 mesophilic biogas reactor fed with manure. Cattle manure was collected from an  
136 operating biogas reactor's manure storage at the Deutsches  
137 Biomasseforschungszentrum, Leipzig, Germany. Swine manure and poultry litter were  
138 collected from local farmers and stored at 5 °C for one month before experiment start.  
139 The manure reactors were supplemented with either 5:1 mM TA-NaF or 1% (w/w) LS  
140 as treatments prior to incubation. All reactor setups were performed in duplicates.

141 **2.2.2 Sampling and analyzes of manure batch reactors.** The headspace pressure  
142 development was measured frequently with a LEO 5 digital manometer (Omni  
143 instruments, Dundee, UK), and samples for biogas composition and compound-specific  
144 isotope analysis were collected from the headspace and stored as described for the  
145 maize silage reactors. After gas sampling, the headspace was flushed with nitrogen for 1  
146 minute at ~5 L min<sup>-1</sup> via syringe needles through rubber septa. The pH, TAN, VFA, VS,

147 TS, and samples for microbial community analysis were collected as described for the  
148 maize silage reactors.

149

## 150 2.3 Chemical analysis

151 Biogas composition was analyzed on a Clarius 580 GC system (PerkinElmer,  
152 Washington, USA) using a 7' HayeSep N 60/80, 1/8" Sf column followed by a 9'  
153 Molecular Sieve 13x mesh 45/60, OD 1/8" using a thermal conductivity detector  
154 (Agilent Technologies, Germany). Samples for VFA analysis were esterified as  
155 described in Mulat, D. et al., (Mulat et al., 2016) and analyzed on a GC 7890A GC  
156 System (Agilent Technologies, Germany) equipped with a DB-FFAP column (Agilent  
157 technologies, Germany) (length 60 m, ID 0.25 mm and film thickness of 0.5  $\mu\text{m}$ ) and a  
158 flame ionization detector (Agilent Technologies, Germany). Total VFA was calculated  
159 as the sum of C1-C10 linear carboxylic acids, lactic acid, benzoic acid, phenylacetic  
160 acid, and phenylpropanoic acid. For TAN analysis, samples were diluted in  
161 demineralized water (1000 – 4000 times) and determined by the standard Nessler  
162 method using a DR 3900 benchtop spectrometer (Hach-Lange, Loveland, CO, USA)  
163 (Koch and McMeekin, 1924). The VS and TS were determined gravimetrically by  
164 heating at 105 °C (Binder oven, Germany) for 24 h followed by burning at 550 °C  
165 (P300 Nabertherm furnace, Germany) for 6 h. The sugar content in lignosulfonic acid  
166 was determined according to (Sluiter et al., 2012).

167

## 168 2.4 Compound-specific isotope analysis

169 The  $\delta^{13}\text{C}$  isotope signature was analyzed by gas chromatography-combustion-isotope  
170 ratio mass spectrometry (GC/C/IRMS). A GC 7890A (Agilent Technologies, Germany)

171 equipped with a GC IsoLink interface coupled via a ConFlo IV open split system to a  
 172 MAT 253 IRMS (Thermo Scientific, Waltham, Massachusetts, USA) was used.  
 173 Samples of 0.2 to 1.0 mL headspace were injected with a split ratio of 1:5.  
 174 Chromatographic separation was done on a PoraBOND Q column (50 m length, 0.32  
 175 mm inner diameter, 5  $\mu$ m film thickness; Agilent technologies, Germany) at a constant  
 176 helium carrier gas flow of 2.0 mL/min with the following temperature program: 40  $^{\circ}$ C  
 177 (hold 120 min isotherm); increasing at a 20  $^{\circ}$ C min<sup>-1</sup> rate to 250  $^{\circ}$ C (hold 10 min  
 178 isotherm). The injector temperature was set to 250  $^{\circ}$ C. The bulk  $\delta^{13}$ C signatures of  
 179 cellulose, TA, LS, and urea were measured with an elemental analyzer - isotope ratio  
 180 mass spectrometry system (EA-IRMS) as described in Supplementary materials.  
 181 Stable carbon isotope ratios were reported as delta notations relative to the international  
 182 standard Vienna Pee Dee Belemnite (VPDB) (Coplen, 2011; Werner and Brand, 2001).

$$183 \quad \delta^{13}\text{C} = \left( \frac{{}^{13}\text{C}/{}^{12}\text{C}(\text{sample})}{{}^{13}\text{C}/{}^{12}\text{C}(\text{VPDB})} - 1 \right) \quad (1)$$

184 The isotope fractionation factor,  $\alpha_{AB}$ , for the reaction,  $A \rightarrow B$ , is defined according to  
 185 (Conrad, 2005).

$$186 \quad \alpha_{AB} = (\delta A + 1000) / (\delta B + 1000) \quad (2)$$

187 Alternatively, isotope fractionation can be expressed as an enrichment factor (Conrad,  
 188 2005),  $\epsilon_{AB}$ , as:

$$189 \quad \epsilon_{AB} = (1 - \alpha_{AB}) \cdot 10^3 \quad (3)$$

190 However, the apparent fractionation factor,  $\alpha_c$ , between  $\text{CO}_2$  and  $\text{CH}_4$  (Conrad, 2005;  
 191 Whiticar, 1999) is more convenient to use when dealing with mixed cultures:

192  $\alpha_c = (\delta^{13}\text{C}_{\text{CO}_2} + 1000)/(\delta^{13}\text{C}_{\text{CH}_4} + 1000)$  (4)

193 If  $\delta^{13}\text{C}_{\text{CO}_2} - \delta^{13}\text{C}_{\text{CH}_4} < 100\text{‰}$ , the equivalent apparent enrichment factor,  $\epsilon_c$ , can be  
194 approximated (Conrad, 2005; Fry, 2003) as:

195  $\epsilon_c \approx \delta^{13}\text{C}_{\text{CO}_2} - \delta^{13}\text{C}_{\text{CH}_4}$  (5)

196 Hydrogenotrophic methanogenesis displays larger isotope fractionation than  
197 acetoclastic methanogenesis, yielding more depleted (negative)  $\delta^{13}\text{C}_{\text{CH}_4}$  values (Conrad,  
198 2005). Thus, characteristic  $\epsilon_c$  values for hydrogenotrophic methanogenesis and  
199 acetoclastic methanogenesis dominated environments are  $\epsilon_c > 65\text{‰}$  and  $\epsilon_c < 55\text{‰}$ ,  
200 respectively (Conrad, 2005; Whiticar, 1999).

201

## 202 2.5 Microbial community analysis

203 **2.5.1 DNA extraction.** Samples were defrosted and 400-500 mg were used to extract  
204 DNA using a NucleoSpin soil kit (Macherey-Nagel GmbH & Co. KG, Düren,  
205 Germany). The DNA quality was checked with a 0.8% agarose gel electrophoresis, and  
206 the DNA concentration was determined using a NanoDrop ND-1000 UV/visible  
207 spectral photometer (PiqLab, Germany) and a Qubit dsDNA BR Assay kit (Invitrogen,  
208 Waltham Massachusetts, USA).

209 **2.5.2 Amplicon sequencing of 16S rRNA and mcrA.** The bacterial community  
210 structure was assessed by PCR amplifying the V3-V4 variable regions of the archaeal  
211 and bacterial 16S rRNA gene using the 341f (5'-CCTACGGGNGGCWGCAG-3') and  
212 785r (5'-GACTACHVGGGTATCTAATCC-3') primer set (Klindworth et al., 2013).  
213 The methanogenic community structure was assessed by PCR amplifying the methyl  
214 coenzyme reductase A gene (mcrA) by using the mlas (GGTGGTGTMGGD  
215 TTCACMCARTA) and mcrA-rev (CGTTCATBGCCTAGTTVGGRTAGT) primer set

216 (Steinberg and Regan, 2008). The PCR products were purified with Agencourt AMPure  
217 XP magnetic beads and a magnetic stand (Beckman Coulter, Brea, California, USA).  
218 An index PCR on the purified PCR products was carried out using a Nextera XT  
219 DNA Library Preparation Kit (Illumina, San Diego, Californien, USA). The  
220 cleaned index PCR products were diluted and sequenced with the Illumina MiSeq  
221 amplicon sequencer (Illumina V3, 2X300bp).

222

## 223 2.6 Data analysis and statistics

224 **2.6.1 Microbial community data analysis.** For 16S rRNA and mcrA gene sequencing,  
225 the raw sequencing data was processed in QIIME2 bioinformatics platform 2018.11  
226 (Bolyen et al., 2018). Denoising of paired-end reads, dereplication, chimera filtering,  
227 and generation of Amplicon Sequence Variants (ASVs) were made with the DADA2  
228 plugin according to instructions in (Callahan et al., 2016). For 16S rRNA the taxonomy  
229 was assigned to the ASVs using the MiDAS 2.1.3 reference database built for the V3 –  
230 V4 hypervariable regions, respectively (McIlroy et al., 2015). The methanogen  
231 taxonomy was assigned using a custom database of mcrA genes (Popp et al., 2017). For  
232 the 16S rRNA and mcrA amplicons, the amplicon sequence variants frequency table,  
233 taxonomy, and DNA sequences were exported from QIIME2 objects to text and FASTA  
234 files for data analysis. Non-metric multidimensional scaling plots were generated in R  
235 (R Core Team, Vienna, Austria) using the vegan package and the “envfit” function.

236 **2.6.2 Statistics.** Errors reported in tables and figures are presented as sample standard  
237 deviations, and statistical significances were based one-way ANOVA with a Tukeys  
238 HSD post hoc test to test pairwise differences between group means. For one-way

239 ANOVA and Tukeys HSD the level of significance ( $\alpha$ ) was 0.05. The statistical tests  
240 were done in Microsoft Excel 2016.

241

## 242 3. Results and Discussion

### 243 3.1 Chemical characterization

244 **3.1.1 Maize silage digestate batch reactors.** The characterization of the maize silage  
245 digestate is shown in Table 1 at experiment initialization (day 0) and end (day 30). The  
246 TAN increased considerably for LS, 10:1 mM TA-NaF, and urea treated reactors from  
247 after 30 days compared to the control reactors (Inoc+sub) (batch 1). This TAN  
248 increment was clearly a consequence of urea hydrolysis. The acetic acid concentration  
249 in 10:1 mM TA-NaF treated samples increased to 4250 mg/L by day 30. This indicated  
250 sustained acetate production and concurrent inhibition of syntrophic acetate oxidation  
251 and acetoclastic methanogenesis. The acetic acid content of urea amended control  
252 reactors increased by day 30 and was significantly higher than the acetic acid content in  
253 reactors with urea+LS (batch 1). This suggests that LS counteracted the urea induced  
254 ammonia inhibition of methanogenesis.

255 **3.1.2 Manure batch reactors.** The characterization of the swine manure, cattle manure  
256 and poultry litter, which were prediluted to the same initial volatile solids content, is  
257 shown in Table 2 at experiment initialization (day 0) and end (day 30). In Table 2, the  
258 acetic acid concentrations were generally higher for reactors incubated at room  
259 temperature. Treatment with TA-NaF decreased the acetic acid content in the poultry  
260 litter batch reactors, contrasting the increase of acetic acid in the swine and cattle  
261 manure batch reactors. Nevertheless, high acetic acid content in the poultry litter control  
262 and poultry litter+LS reactors were observed. Hence, it was speculated that acetic acid

263 accumulation resulted from a lack of methanogenic communities in the poultry litter.  
264 Methanogens have only been reported in poultry excreta in a few studies (Miller et al.,  
265 1986; Saengkerdsub et al., 2007), and the high TAN content in the undiluted poultry  
266 litter of 6.8 g/L combined with a relatively aerobic environment in poultry litter could  
267 limit the initial abundance of methanogens in the poultry litter reactors. Low acetic acid  
268 concentration in poultry litter+TA-NaF reactors, suggested that microbial inhibition  
269 possibly affected acetogenic and acidogenic bacteria, which normally produce acetate  
270 and other VFAs. However, the slight TAN increment in the TA-NaF inhibited poultry  
271 litter by day 30 was indicative of a sustained uric acid and urea hydrolysis activity. The  
272 environmental parameters in general portrayed similar tendencies for swine and cattle  
273 manure digestion. The environmental parameters for poultry litter diverged from those  
274 of swine and cattle manure, which was attributed to the lack of methanogenic activity.

275

## 276 3.2 Methane production

277 **3.2.1 Maize silage digestate batch reactors.** The methane production was measured  
278 from biogas slurry with cellulose as standard substrate under the influence of urea, TA-  
279 NaF, and LS addition. The methane recovery in all positive control reactors (Inoc+sub)  
280 were  $83.1 \pm 6.5\%$  of the theoretical methane yields according to Boyles extended  
281 formula, refined from (Buswell and Mueller, 1952). In Figure 2a, the methane yield of  
282 the positive urea control (inoc+cellulose+urea) was significantly lower than the positive  
283 control ( $1488 \pm 26$  mL vs  $1863 \pm 19$  mL), indicating urea induced inhibition of the  
284 methanogenic activity (Lv et al., 2018). Interestingly, in the presence of LS, the urea  
285 inhibiting effect on methanogenesis was counteracted yielding  $1867 \pm 44$  mL methane.  
286 This could be explained by either inhibition of urea hydrolysis to ammonia or chelation

287 of ammonium ions by LS. The latter theory was rejected from rough estimates of a LS  
288 chelating capacity of 3.5 mmole cations/g LS, which is insignificant in comparison to  
289 the total abundance of cations in the batch reactors. The methane spike, observed within  
290 the first 24 hours from LS supplemented reactors (Fig. 2b), was attributed to  
291 degradation of simple sugars (Glucose + galactose + xylose) contained in the LS  
292 powder (16% of the LS). The 10:1 mM TA-NaF treatment completely inhibited  
293 methanogenic activity (Fig. 2a). However, 5:1 mM TA-NaF amended reactors without  
294 cellulose substrate (Fig. 2b) produced  $602 \pm 23$  mL extra methane compared to the  
295 inoculum control from day 7 to day 30, suggesting microbial degradation of TA. Based  
296 on Figure 2, it was concluded that TA-NaF supplementation was unsuited as treatment  
297 for ammonia inhibited AD given the general negative or delaying effect on methane  
298 production. Moreover, the biogas quality of TA-NaF amended reactors (Fig. 2a) were  
299 poor (35:65 methane:carbon dioxide ratio) compared to other treatments (Fig. 2a), with  
300 final methane:carbon dioxide ratios around 65:35 (Supplementary materials).  
301 Nevertheless, TA-NaF utilization for reducing methane production would be beneficial  
302 in manure storage tanks, storage of AD digestate used as fertilizer, and in livestock  
303 buildings.

304 **3.2.2 Manure batch reactors.** To investigate the potential of TA-NaF as methane  
305 mitigation agent in a manure storage scenario, TA-NaF was added to reactors with  
306 swine manure, cattle manure, or poultry litter. Although LS was not expected to  
307 mitigate methanogenic activity, it was included as a treatment for comparative purposes.  
308 The methane production from the manure batch reactors are shown in Figure 3.  
309 Methane production was greater at 38 °C for all manure types, as expected from  
310 methanogen growth rate studies (Lin et al., 2016). The methane production was delayed

311 only briefly in swine manure with 5:1 mM TA-NaF at 38 °C and resulted in final yields  
312 equal to or exceeding the untreated controls. This is consistent with the observations of  
313 TA degradation in 5:1 mM TA-NaF treated maize silage reactors (Fig. 2b). Treatment  
314 with TA-NaF, inhibited methane production more efficiently in cattle manure than in  
315 swine manure at both temperatures, suggesting a less resilient microbial community in  
316 the cattle manure. This finding highlights the potential relevance of using TA-NaF as a  
317 methane-mitigating agent in cattle manure. Reactors with LS exceeded the methane  
318 yields of the untreated swine manure control at both incubation temperatures. This trend  
319 occurred concordantly with the high TAN concentration in the swine manure (Table 2),  
320 which supports the observed counteractive effect of LS on urea hydrolysis to ammonia.  
321 A similar effect of LS was not observed in cattle manure, which did not contain nearly  
322 as high TAN concentrations either. One of the reactors with poultry litter and LS at 38  
323 °C produced significant amounts of methane (354 mL) from day 17 to 28, whereas the  
324 remaining parallel reactors inoculated with poultry litter produced less than 1 mL  
325 methane during the entire experiment. This suggested a very limited methanogen  
326 population in the poultry litter inoculum at experiment start or an extremely long lag  
327 phase of the methanogens to accommodate to the conditions in poultry litter batch  
328 reactors.

329

### 330 3.3 Carbon isotope signatures

331 Carbon isotope signatures were measured as a proxy for the relative contribution of  
332 acetoclastic and hydrogenotrophic methanogenesis (Conrad, 2005), as described in  
333 section 2.4. By conducting compound specific isotope analysis, further insight into the  
334 effect of TA-NaF and LS was acquired.

335 **3.3.1 Maize silage digestate batch reactors.** In Figure 4, the  $\delta^{13}\text{C}$  signatures are  
336 presented for batch 1 (Fig. 4a) and batch 2 (Fig. 4b) reactors. The relatively negative  
337  $\delta^{13}\text{C}_{\text{CO}_2}$  signatures of urea amended reactors (Fig. 4a) were likely related to ureolytic  
338 activity characterized by an isotope enrichment factor of around 12.5‰ (Millo et al.,  
339 2012), and the fact that the urea was already  $^{13}\text{C}$  depleted ( $\delta^{13}\text{C} = -41\text{‰}$ ) compared to  
340 the cellulose ( $\delta^{13}\text{C} = -24.9\text{‰}$ ). For  $\delta^{13}\text{C}_{\text{CH}_4}$ , the urea amended reactors (Fig. 4a) were  
341 also relatively depleted, indicating dominance of hydrogenotrophic methanogenesis  
342 (Conrad, 2005; Nikolausz et al., 2013). However, with urea + 10:1 mM TA:NaF  
343 treatment (Fig. 4a), the  $\delta^{13}\text{C}_{\text{CH}_4}$  values reached as low as -82‰ after 27 days, indicating  
344 that TA-NaF inhibited acetoclastic methanogenesis in addition to the urea induced  
345 ammonia inhibition of acetoclastic methanogenesis. In comparison, Figure 4b shows  
346  $\delta^{13}\text{C}_{\text{CH}_4}$  values around -30‰ to -35‰ for the 5:1 mM TA:NaF reactors, coinciding with  
347 the period where methane was produced (see Fig. 2b). Hence, bacterial degradation of  
348 TA that fueled acetoclastic methanogenesis must have occurred. However, at high TA  
349 concentrations, complete inhibition of acetoclastic methanogenesis probably results in  
350 acetate accumulation, as reported in Table 1. Lignosulfonic acid seemed to affect  
351  $\delta^{13}\text{C}_{\text{CH}_4}$  values in the positive direction compared to the urea controls (inoc+sub+urea in  
352 Fig. 4a). Hydrogenotrophic methanogen predominance has previously been observed  
353 under inhibitory or otherwise environmental stressing conditions (Buhlmann et al.,  
354 2019; Webster et al., 2016), supporting the deductions made here. The  $\delta^{13}\text{C}$  signatures  
355 of TA and LS are -27.5‰ and -28.5‰, respectively, closely resembling the  $\delta^{13}\text{C}$   
356 signature of cellulose, and thereby ruling out their potential contribution to the depleted  
357  $\delta^{13}\text{C}$  values.

358 **3.3.2 Manure batch reactors.** Carbon signatures in the manure batch reactors were  
359 measured to evaluate whether the observations from the maize silage digestate batch  
360 reactors were associated with the inoculum. As presented in Figure 4c, clear differences  
361 in carbon isotope signatures were measured for the different manure types. Carbon  
362 dioxide from swine manure reactors was significantly enriched in  $^{13}\text{C}$  compared to the  
363 carbon dioxide from cattle manure reactors and poultry litter reactors ( $\delta^{13}\text{C}_{\text{CO}_2}$  of  $19.81$   
364  $\pm 0.87\%$  for swine manure vs  $-9.64 \pm 1.02\%$  for cattle manure and poultry litter, errors  
365 as 95% confidence intervals). Only a few samples with TA-NaF treatment were  
366 measurable due to extremely limited quantities of biogas produced in these reactors.  
367 Cattle and swine manure reactors incubated at room temperature yielded more negative  
368  $\delta^{13}\text{C}_{\text{CH}_4}$  values, and hence yielded larger  $\epsilon_c$  than cattle and swine manure reactors  
369 incubated at  $38^\circ\text{C}$ . Based upon  $\epsilon_c$ , swine manure reactors were dominated by  
370 hydrogenotrophic methanogenesis regardless of incubation temperature. Mostly,  
371 hydrogenotrophic methanogenesis was dominant in cattle manure reactors incubated at  
372 room temperature, while in poultry litter reactors the dominant pathway was acetoclastic  
373 methanogenesis.. The latter finding was unexpected, considering the fact that biogas  
374 from poultry manure fed AD is normally characterized by more depleted  $\delta^{13}\text{C}_{\text{CH}_4}$   
375 values, which indicate the predominance of hydrogenotrophic methanogens (Nikolausz  
376 et al., 2013). In general, LS and TA-NaF supplemented manure reactors were  
377 characterized by slightly more negative  $\delta^{13}\text{C}$  signatures compared to the untreated  
378 manure reactors. The seemingly small effect of TA-NaF and LS on  $\delta^{13}\text{C}$  signatures  
379 suggested that the methanogenic community was already dominated by  
380 hydrogenotrophic methanogens, possibly as a consequence of adaptation to the naturally  
381 high TAN concentrations in manure. Another explanation is that the gut conditions of

382 these animals do not support acetoclastic methanogenesis, therefore such methanogens  
383 are negligible in the manure (Ozbayram et al., 2020).

384

### 385 3.4 Microbial community analysis

386 A dual approach was used for the microbial community structure analysis by targeting  
387 both the *mcrA* and 16S rRNA genes. The *mcrA* gene approach strictly targets  
388 methanogens, as this gene is unique to this group of microorganism (Friedrich, 2005).

389 On the other hand, the domain-specific 16S rRNA gene is ubiquitous in all bacteria and  
390 archaeal cells, and hence is not restricted to only methanogens (Janda and Abbott,  
391 2007).

392 **3.4.1 Methanogens in maize silage digestate batch reactors.** Figure 5 shows the non-  
393 metric multidimensional scaling (NMDS) plot (Fig. 5a) and the relative abundance of  
394 methanogens (Fig. 5b). *Methanoculleus* and *Methanotherix* (formerly *Methanosaeta*)  
395 were highly represented in all samples (Fig 5b). The acetoclastic genus *Methanotherix*  
396 (Holmes and Smith, 2016) was negatively correlated with TA-NaF, whereas  
397 *Methanogenium* and methanogens belonging to the class of Thermoplasmata was  
398 positively correlated with TA-NaF. The latter methanogenic lineages exhibit both  
399 hydrogenotrophic and methylotrophic methanogenesis and is consistent with the  
400 depleted  $\delta^{13}\text{C}_{\text{CH}_4}$  values observed with TA-NaF treatment (Fig 4a). The genus  
401 *Methanoculleus* was more tolerant to high urea and TAN concentrations. Both  
402 *Methanoculleus* and *Methanogenium* genera belong to the Methanomicrobiaceae  
403 family, which has shown to be resilient to environmental stress and ammonia inhibition  
404 (Bonk et al., 2018; Esquivel-Elizondo et al., 2016).

405 **3.4.2 Methanogens in manure batch reactors.** Figure 6 shows the non-metric  
406 multidimensional scaling plot (Fig. 6a) and the relative abundance (Fig. 6b) of  
407 methanogens in manure batch reactors. The methanogen community structure was  
408 correlated with manure type rather than manure treatment. Swine manure was  
409 dominated by *Methanoculleus* and Thermoplasmata, whereas cattle manure was  
410 dominated by *Methanocorpusculum* and various genera belonging to the  
411 Methanomassiliicoccus order. The Methanomassiliicoccus order is taxonomically  
412 classified under Thermoplasmata and rely on an external H<sub>2</sub> source to reduce methyl-  
413 compounds to methane (Borrel et al., 2014). Methanomassiliicoccales was previous  
414 found to be abundant in the rumen fluid (Ozbayram et al., 2020) and the results  
415 presented here support and highlight the significance of hydrogen dependent  
416 methylotrophic methanogenesis in manure as well. Methylotrophic methanogenesis  
417 carried out by *Methanosarcina* species are characterized by large fractionation factors  
418 (Penger et al., 2012), and hence it is likely that the large apparent fractionation factors  
419 of swine and cattle manure (Fig. 4c) were to a significant degree a consequence of  
420 hydrogen dependent methylotrophic methanogenesis. Methanogens in poultry litter  
421 were assigned to Thermoplasmata (Fig. 6b) but this correlation was not significant (Fig.  
422 6a) and methanogens were only detected in some of the poultry litter reactors. The low  
423 abundance or absence of methanogens in poultry litter reactors is consistent with the  
424 minimal or absent methane yields (Fig. 3).

425 **3.4.3 Bacteria in maize silage digestate and manure batch reactors.** In maize silage  
426 digestate, *Fastidiosipila*, *Hydrogenisporalis*, Ruminococcaceae, and VadimBC27  
427 wastewater sludge group was dominant (Supplementary materials). *Fastidiosipila* and  
428 *Hydrogenisporalis* decreased with TA-NaF treatment, whereas VadimBC27 wastewater

429 sludge group and Ruminococcaceae were more resilient to TA-NaF. Ruminococcaceae  
430 is found in animal gut systems and is suited to degrade recalcitrant plant materials  
431 (Biddle et al., 2013) possibly explaining its adaption to TA-NaF. For swine manure  
432 VadimBC27 wastewater sludge group and *Clostridium senso stricto 1* were dominant  
433 taxa (Supplementary materials). In cattle manure *Sphaerochaeta*, *Proteiniphilum*, and  
434 *Acholeplasma* were abundant genera (Supplementary materials). *Acholeplasma*  
435 abundance in cattle manure was substantially reduced with TA-NaF treatment and  
436 replaced by *Pseudobutyrvibrio* at 38 °C (Supplementary materials). *Pseudobutyrvibrio*  
437 ferments carbohydrates to lactic and butyric acid, which was also reflected in the high  
438 VFA content seen in Table 2. Poultry litter was dominated by *Ruminoclostridium 5* at  
439 38 °C and by *Bacteroides* at 23 °C (Supplementary materials). There was no significant  
440 correlation with LS treatment for any of the manure types. In general, *Clostridium senso*  
441 *stricto 1* and VadimBC27 wastewater sludge group were the taxa mostly correlated with  
442 TA-NaF treatment (Supplementary materials), which suggest better adaptation  
443 capabilities of these microbial groups. Most of the microbial groups were affiliated to  
444 taxa without cultured members. This highlights the importance of further exploration of  
445 the microbial diversity in anaerobic digestion systems.

446

#### 447 4. Conclusion

448 Lignosulfonic acid (LS) could be a promising supplement to anaerobic digesters  
449 suffering from urea induced methanogenesis inhibition. This statement is linked to a  
450 lesser inhibition of acetoclastic methanogens upon high urea loads in anaerobic  
451 digestion. Tannic acid with fluoride impairs methane production at high concentrations  
452 and is suitable for mitigating methane emissions from manure storages. *Methanotherix*

453 was very susceptible to TA-NaF inhibition, whereas hydrogenotrophic methanogens  
454 were more resilient to TA-NaF treatment. These observations strongly suggest that the  
455 methanogen community influences the efficacy of both LS and TA-NaF treatment on  
456 the anaerobic digestion process.

## 457 Acknowledgements

458 The authors thank Bruna Grosch Schroeder, Washington Logroño, Ute Lohse and  
459 Natália Hachow Motta dos Passos for assistance in the laboratory. Funding: This work  
460 was supported by GUDP under the Danish AgriFish Agency, Ministry of Environment  
461 and Food Denmark (Grant 34009-15-0934).

## 462 Appendix A. Supplementary materials

463 E-supplementary materials for this work can be found in e-version of this paper online

## 464 References

- 465 Al-Jumaili, W.S., Goh, Y.M., Jafari, S., Rajion, M.A., Jahromi, M.F., Ebrahimi, M.,  
466 2017. An in vitro study on the ability of tannic acid to inhibit methanogenesis and  
467 biohydrogenation of C18 PUFA in the rumen of goats. *Ann. Anim. Sci.* 17, 491–  
468 502. <https://doi.org/10.1515/aoas-2016-0059>
- 469 Biddle, A., Stewart, L., Blanchard, J., Leschine, S., 2013. Untangling the genetic basis  
470 of fibrolytic specialization by lachnospiraceae and ruminococcaceae in diverse gut  
471 communities. *Diversity* 5, 627–640. <https://doi.org/10.3390/d5030627>
- 472 Bolyen, E., Dillon, M., Bokulich, N., Abnet, C., Al-Ghalith, G., Alexander, H., Alm, E.,  
473 Arumugam, M., Asnicar, F., Bai, Y., Bisanz, J., Bittinger, K., Brejnrod, A.,

474 Brislawn, C., Brown, T., Callahan, B., Chase, J., Cope, E., Dorrestein, P., Douglas,  
475 G., Durall, D., Duvallet, C., Edwardson, C., Ernst, M., Estaki, M., Fouquier, J.,  
476 Gauglitz, J., Gibson, D., Gonzalez, A., Gorlick, K., Guo, J., Hillmann, B., Holmes,  
477 S., Holste, H., Huttenhower, C., Huttley, G., Janssen, S., Jarmusch, A., Jiang, L.,  
478 Kaehler, B., Keefe, C., Keim, P., Kelley, S., Knights, D., Koester, I., Kosciulek, T.,  
479 Kreps, J., Lee, J., Ley, R., Liu, Y.-X., Lofffield, E., Lozupone, C., Maher, M.,  
480 Marotz, C., Martin, B., McDonald, D., McIver, L., Melnik, A., Metcalf, J.,  
481 Morgan, S., Morton, J., Navas-Molina, J., Orchanian, S., Pearson, T., Peoples, S.,  
482 Petras, D., Pruesse, E., Rivers, A., Robeson, M., Rosenthal, P., Segata, N., Shaffer,  
483 M., Shiffer, A., Sinha, R., Spear, J., Swafford, A., Thompson, L., Torres, P., Trinh,  
484 P., Tripathi, A., Turnbaugh, P., Ul-Hasan, S., Vargas, F., Vogtman, E., Walters,  
485 W., Wan, Y., Wang, M., Warren, J., Weber, K., Willis, A., Zaneveld, J., Zhang, Y.,  
486 Zhu, Q., Knight, R., Caporaso, G., 2018. QIIME 2: Reproducible, interactive,  
487 scalable, and extensible microbiome data science. PeerJ Prepr.  
488 <https://doi.org/10.7287/peerj.preprints.27295>

489 Bonk, F., Popp, D., Weinrich, S., Sträuber, H., Kleinsteuber, S., Harms, H., Centler, F.,  
490 2018. Ammonia Inhibition of Anaerobic Volatile Fatty Acid Degrading Microbial  
491 Communities. *Front. Microbiol.* 9, 1–13. <https://doi.org/10.3389/fmicb.2018.02921>

492 Borrel, G., Parisot, N., Harris, H.M.B., Peyretailade, E., Gaci, N., Tottey, W., Bardot,  
493 O., Raymann, K., Gribaldo, S., Peyret, P., O’Toole, P.W., Brugère, J.F., 2014.  
494 Comparative genomics highlights the unique biology of Methanomassiliicoccales,  
495 a Thermoplasmatales-related seventh order of methanogenic archaea that encodes  
496 pyrrolysine. *BMC Genomics* 15. <https://doi.org/10.1186/1471-2164-15-679>

497 Bravo, L., 2009. Polyphenols: Chemistry, Dietary Sources, Metabolism, and Nutritional  
498 Significance. *Nutr. Rev.* 56, 317–333. [https://doi.org/10.1111/j.1753-](https://doi.org/10.1111/j.1753-4887.1998.tb01670.x)  
499 [4887.1998.tb01670.x](https://doi.org/10.1111/j.1753-4887.1998.tb01670.x)

500 Buhlmann, C.H., Mickan, B.S., Jenkins, S.N., Tait, S., Kahandawala, T.K.A., Bahri,  
501 P.A., 2019. Ammonia stress on a resilient mesophilic anaerobic inoculum:  
502 Methane production, microbial community, and putative metabolic pathways.  
503 *Bioresour. Technol.* 275, 70–77. <https://doi.org/10.1016/j.biortech.2018.12.012>

504 Buswell, A.M., Mueller, H.F., 1952. Mechanism of Methane Fermentation. *Ind. Eng.*  
505 *Chem.* 44, 550–552. <https://doi.org/10.1021/ie50507a033>

506 Callahan, B.J., McMurdie, P.J., Rosen, M.J., Han, A.W., Johnson, A.J.A., Holmes, S.P.,  
507 2016. DADA2: High-resolution sample inference from Illumina amplicon data.  
508 *Nat. Methods* 13, 581–583. <https://doi.org/10.1038/nmeth.3869>

509 Calvo-Flores, F.G., Dobado, J.A., 2010. Lignin as renewable raw material.  
510 *ChemSusChem* 3, 1227–1235. <https://doi.org/10.1002/cssc.201000157>

511 Conrad, R., 2005. Quantification of methanogenic pathways using stable carbon  
512 isotopic signatures: A review and a proposal. *Org. Geochem.* 36, 739–752.  
513 <https://doi.org/10.1016/j.orggeochem.2004.09.006>

514 Coplen, T.B., 2011. Guidelines and recommended terms for expression of stable-  
515 isotope-ratio and gas-ratio measurement results. *Rapid Commun. Mass Spectrom.*  
516 25, 2538–2560. <https://doi.org/10.1002/rcm.5129>

517 Dalby, F.R., Svane, S., Sigurdarson, J.J., Sørensen, M.K., Hansen, M.J., Karring, H.,  
518 Feilberg, A., n.d. Unpublished results. Synergistic Tannic Acid-Fluoride Inhibition

519 of Ammonia Emissions and Simultaneous Reduction of Methane and Odor  
520 Emissions from Livestock Waste.

521 Elzing, A., Monteny, G.J., 1997. Ammonia emission in a scale model of a dairy-cow  
522 house. *Trans. Am. Soc. Agric. Eng.* 40, 713–720.  
523 <https://doi.org/10.13031/2013.21301>

524 Esquivel-Elizondo, S., Parameswaran, P., Delgado, A.G., Maldonado, J., Rittmann,  
525 B.E., Krajmalnik-Brown, R., 2016. Archaea and Bacteria Acclimate to High Total  
526 Ammonia in a Methanogenic Reactor Treating Swine Waste. *Archaea* 2016.  
527 <https://doi.org/10.1155/2016/4089684>

528 Friedrich, M.W., 2005. Methyl-Coenzyme M Reductase Genes: Unique Functional  
529 Markers for Methanogenic and Anaerobic Methane-Oxidizing Archaea. *Methods*  
530 *Enzymol.* 397, 428–442. [https://doi.org/10.1016/S0076-6879\(05\)97026-2](https://doi.org/10.1016/S0076-6879(05)97026-2)

531 Fry, B., 2003. Steady state models of stable isotopic distributions. *Isotopes Environ.*  
532 *Health Stud.* 39, 219–32. <https://doi.org/10.1080/1025601031000108651>

533 Hansen, M.N., Kai, P., Møller, H.B., 2006. Effects of Anaerobic Digestion and  
534 Separation of Pig Slurry on Odor Emission. *Appl. Eng. Agric.* 22, 135–139.

535 Holly, M.A., Larson, R.A., Powell, J.M., Ruark, M.D., Aguirre-Villegas, H., 2017.  
536 Greenhouse gas and ammonia emissions from digested and separated dairy manure  
537 during storage and after land application. *Agric. Ecosyst. Environ.* 239, 410–419.  
538 <https://doi.org/10.1016/j.agee.2017.02.007>

539 Holmes, D.E., Smith, J.A., 2016. Biologically Produced Methane as a Renewable  
540 Energy Source. *Adv. Appl. Microbiol.* 97.

541 <https://doi.org/10.1016/bs.aambs.2016.09.001>

542 Hou, Y., Velthof, G.L., Oenema, O., 2015. Mitigation of ammonia, nitrous oxide and  
543 methane emissions from manure management chains: A meta-analysis and  
544 integrated assessment. *Glob. Chang. Biol.* 21, 1293–1312.  
545 <https://doi.org/10.1111/gcb.12767>

546 Janda, J.M., Abbott, S.L., 2007. 16S rRNA gene sequencing for bacterial identification  
547 in the diagnostic laboratory: Pluses, perils, and pitfalls. *J. Clin. Microbiol.* 45,  
548 2761–2764. <https://doi.org/10.1128/JCM.01228-07>

549 Klindworth, A., Pruesse, E., Schweer, T., Peplies, J., Quast, C., Horn, M., Glöckner,  
550 F.O., 2013. Evaluation of general 16S ribosomal RNA gene PCR primers for  
551 classical and next-generation sequencing-based diversity studies. *Nucleic Acids*  
552 *Res.* 41, 1–11. <https://doi.org/10.1093/nar/gks808>

553 Koch, F.C., McMeekin, T.L., 1924. A new direct nesslerization micro-kjeldahl method  
554 and a modification of the nessler-folin reagent for ammonia. *J. Am. Chem. Soc.* 46,  
555 2066–2069. <https://doi.org/10.1021/ja01674a013>

556 Lee, X., Turner, P.A., Chen, Z., Baker, J.M., Griffis, T.J., Wood, J.D., Millet, D.B.,  
557 Venterea, R.T., 2017. Nitrous oxide emissions are enhanced in a warmer and  
558 wetter world. *Proc. Natl. Acad. Sci.* 114, 12081–12085.  
559 <https://doi.org/10.1073/pnas.1704552114>

560 Lin, Q., De Vrieze, J., He, G., Li, X., Li, J., 2016. Temperature regulates methane  
561 production through the function centralization of microbial community in  
562 anaerobic digestion. *Bioresour. Technol.* 216, 150–158.  
563 <https://doi.org/10.1016/j.biortech.2016.05.046>

564 Lv, Z., Jiang, J., Liebetrau, J., Richnow, H.H., Fischer, A., Ács, N., Nikolausz, M.,  
565 2018. Ammonium Chloride vs Urea-Induced Ammonia Inhibition of the Biogas  
566 Process Assessed by Stable Isotope Analysis. *Chem. Eng. Technol.* 41, 671–679.  
567 <https://doi.org/10.1002/ceat.201700482>

568 Lv, Z., Leite, A.F., Harms, H., Glaser, K., Liebetrau, J., Kleinstaubler, S., Nikolausz, M.,  
569 2019. Microbial community shifts in biogas reactors upon complete or partial  
570 ammonia inhibition. *Appl. Microbiol. Biotechnol.* 103, 519–533.  
571 <https://doi.org/10.1007/s00253-018-9444-0>

572 McIlroy, S.J., Saunders, A.M., Albertsen, M., Nierychlo, M., McIlroy, B., Hansen,  
573 A.A., Karst, S.M., Nielsen, J.L., Nielsen, P.H., 2015. MiDAS: The field guide to  
574 the microbes of activated sludge. *Database* 2015, 1–8.  
575 <https://doi.org/10.1093/database/bav062>

576 Miller, T.L., Wolin, M.J., Kusel, E.A., 1986. Isolation and characterization of  
577 methanogens from animal feces. *Syst. Appl. Microbiol.* 8, 234–238.  
578 [https://doi.org/10.1016/S0723-2020\(86\)80084-4](https://doi.org/10.1016/S0723-2020(86)80084-4)

579 Millo, C., Dupraz, S., Ader, M., Guyot, F., Thaler, C., Foy, E., Ménez, B., 2012. Carbon  
580 isotope fractionation during calcium carbonate precipitation induced by ureolytic  
581 bacteria. *Geochim. Cosmochim. Acta* 98, 107–124.  
582 <https://doi.org/10.1016/j.gca.2012.08.029>

583 Mulat, D., Jacobi, H., Feilberg, A., Adamsen, A., Richnow, H., Nikolausz, M., 2016.  
584 Changing Feeding Regimes To Demonstrate Flexible Biogas Production: Effects  
585 on Process Performance, Microbial Community Structure, and Methanogenesis  
586 Pathways. *Appl. Environ. Microbiol.* 82, 438–449.

587 <https://doi.org/10.1128/AEM.02320-15>.Editor

588 Nikolausz, M., Walter, R.F.H., Sträuber, H., Liebetrau, J., Schmidt, T., Kleinsteuber, S.,  
589 Bratfisch, F., Günther, U., Richnow, H.H., 2013. Evaluation of stable isotope  
590 fingerprinting techniques for the assessment of the predominant methanogenic  
591 pathways in anaerobic digesters. *Appl. Microbiol. Biotechnol.* 97, 2251–2262.  
592 <https://doi.org/10.1007/s00253-012-4657-0>

593 Ozbayram, E.G., Kleinsteuber, S., Nikolausz, M., 2020. Biotechnological utilization of  
594 animal gut microbiota for valorization of lignocellulosic biomass. *Appl. Microbiol.*  
595 *Biotechnol.* 104, 489–508. <https://doi.org/10.1007/s00253-019-10239-w>

596 Papuc, C., Goran, G. V., Predescu, C.N., Nicorescu, V., Stefan, G., 2017. Plant  
597 Polyphenols as Antioxidant and Antibacterial Agents for Shelf-Life Extension of  
598 Meat and Meat Products : Classification , Structures , Sources , and Action  
599 Mechanisms. *Compr. Rev. Food Sci. Food Saf.* 16, 1243–1268.  
600 <https://doi.org/10.1111/1541-4337.12298>

601 Penger, J., Conrad, R., Blaser, M., 2012. Stable carbon isotope fractionation by  
602 methylotrophic methanogenic archaea. *Appl. Environ. Microbiol.* 78, 7596–7602.  
603 <https://doi.org/10.1128/AEM.01773-12>

604 Popp, D., Plugge, C.M., Kleinsteuber, S., Harms, H., Heike, S., 2017. Inhibitory Effect  
605 of Coumarin on Syntrophic Fatty Acid-Oxidizing and Methanogenic Cultures and  
606 Biogas Reactor Microbiomes. *Appl. Environ. Microbiol.* 83, 1–14.

607 Quideau, S., Deffieux, D., Douat-Casassus, C., Pouységu, L., 2011. Plant polyphenols:  
608 Chemical properties, biological activities, and synthesis. *Angew. Chemie - Int. Ed.*  
609 50, 586–621. <https://doi.org/10.1002/anie.201000044>

610 Saengkerdsub, S., Anderson, R.C., Wilkinson, H.H., Kim, W.K., Nisbet, D.J., Ricke,  
611 S.C., 2007. Identification and quantification of methanogenic archaea in adult  
612 chicken ceca. *Appl. Environ. Microbiol.* 73, 353–356.  
613 <https://doi.org/10.1128/AEM.01931-06>

614 Sierra-Alvarez, R., 2007. The methanogenic toxicity of wastewater lignins and lignin  
615 related compounds. *J. Chem. Technol.* 13, 485–455.  
616 <https://doi.org/10.1002/jctb.280500403>

617 Sluiter, A., Hames, B., Ruiz, R., Scarlata, C., Sluiter, J., Templeton, D., Crocker, D.,  
618 2012. NREL/TP-510-42618 analytical procedure - Determination of structural  
619 carbohydrates and lignin in Biomass, Laboratory Analytical Procedure (LAP).  
620 <https://doi.org/NREL/TP-510-42618>

621 Sørensen, P., Amato, M., 2002. Remineralisation and residual effects of N after  
622 application of pig slurry to soil. *Eur. J. Agron.* 16, 81–95.  
623 [https://doi.org/10.1016/S1161-0301\(01\)00119-8](https://doi.org/10.1016/S1161-0301(01)00119-8)

624 Steinberg, L.M., Regan, J.M., 2008. Phylogenetic Comparison of the Methanogenic  
625 Communities from an Acidic , Oligotrophic Fen and an Anaerobic Digester  
626 Treating Municipal Wastewater Sludge. *Appl. Environ. Microbiol.* 74, 6663–6671.  
627 <https://doi.org/10.1128/AEM.00553-08>

628 Sun, C., Cao, W., Banks, C.J., Heaven, S., Liu, R., 2016. Biogas production from  
629 undiluted chicken manure and maize silage: A study of ammonia inhibition in high  
630 solids anaerobic digestion. *Bioresour. Technol.* 218, 1215–1223.  
631 <https://doi.org/10.1016/j.biortech.2016.07.082>

632 Webster, T.M., Smith, A.L., Reddy, R.R., Pinto, A.J., Hayes, K.F., Raskin, L., 2016.

- 633 Anaerobic microbial community response to methanogenic inhibitors 2-  
634 bromoethanesulfonate and propynoic acid. *Microbiologyopen* 5, 537–550.  
635 <https://doi.org/10.1002/mbo3.349>
- 636 Werner, R.A., Brand, W.A., 2001. Referencing strategies and techniques in stable  
637 isotope ratio analysis. *Rapid Commun. Mass Spectrom.* 15, 501–519.  
638 <https://doi.org/10.1002/rcm.258>
- 639 Westerman, P.W., Bicudo, J.R., 2005. Management considerations for organic waste  
640 use in agriculture. *Bioresour. Technol.* 96, 215–221.  
641 <https://doi.org/10.1016/j.biortech.2004.05.011>
- 642 Whitehead, T.R., Spence, C., Cotta, M.A., 2013. Inhibition of hydrogen sulfide,  
643 methane, and total gas production and sulfate-reducing bacteria in in vitro swine  
644 manure by tannins, with focus on condensed quebracho tannins. *Appl. Microbiol.*  
645 *Biotechnol.* 97, 8403–8409. <https://doi.org/10.1007/s00253-012-4562-6>
- 646 Whiticar, M.J., 1999. Carbon and hydrogen isotope systematics of bacterial formation  
647 and oxidation of methane. *Chem. Geol.* 161, 291–314.  
648 [https://doi.org/10.1016/S0009-2541\(99\)00092-3](https://doi.org/10.1016/S0009-2541(99)00092-3)
- 649 Wu, C., Liu, J., Zhao, P., Piringer, M., Schaubberger, G., 2016. Conversion of the  
650 chemical concentration of odorous mixtures into odour concentration and odour  
651 intensity: A comparison of methods. *Atmos. Environ.* 127, 283–292.  
652 <https://doi.org/10.1016/j.atmosenv.2015.12.051>

## 653 Figure Captions

654 **Figure 1.** Schematic presentation of experimental work. TA-NaF = tannic acid with  
655 sodium fluoride, LS = lignosulfonic acid, Sub = Substrate (cellulose), GC/IRMS = gas  
656 chromatography combustion isotope ratio mass spectrometry, AMPTS = automatic  
657 methane potential test system.

658 **Figure 2.** Methane potential tests of maize silage batch reactors. The reactors were  
659 amended with tannic acid with sodium fluoride (TA:NaF) or lignosulfonic acid (LS) (10  
660 g/L) in batch experiment 1 **(a)** and batch experiment 2 **(b)**. Curves labeled with the same  
661 letter were not significantly different by experiment end (*p*-value is for ANOVA).

662 **Figure 3.** Methane production from swine manure, cattle manure, and poultry litter.  
663 Manures were incubated at 38 °C and at room temperature (~ 23 °C).

664 **Figure 4.** Isotope signatures of CH<sub>4</sub> and CO<sub>2</sub> from maize silage digestate. Maize silage  
665 digestate from batch experiment 1 **(a)** and batch experiment 2 **(b)**. Inoc=inoculum  
666 (maize silage digestate), Sub=substrate (cellulose), TA:NaF=tannic acid:sodium  
667 fluoride, LS=lignosulfonic acid (10 g/L). Curves labeled with the same letter were not  
668 significantly different by experiment end (*p*-value is for ANOVA). **(c)** Carbon isotope  
669 signatures of CH<sub>4</sub> and CO<sub>2</sub> from manure batch reactors. Dashed lines indicate the  
670 apparent enrichment factor,  $\epsilon_c$ . Time resolution was omitted as there was no significant  
671  $\delta^{13}\text{C}$  development over time. TA-NaF= 5:1 mM tannic acid: sodium fluoride,  
672 LS=lignosulfonic acid (10 g/L). The numbers 23 and 38 indicate incubation  
673 temperatures in °C.

674 **Figure 5.** **(a)** Non-metric multidimensional scaling plots (NMDS) of the methanogenic  
675 community structures in maize silage digestate batch reactors based on *mcrA* amplicon  
676 sequencing. **(b)** Relative abundances of methanogens from batch 1 and batch 2.

677 Sub=substrate (cellulose), TA:NaF=tannic acid:sodium fluoride, LS=lignosulfonic acid  
678 (10 g/L). The taxonomic level in **(a)** and **(b)** is denoted with (s) for species level, (g) for  
679 genus level, (f) for family level, (o) for order level, and (c) for class level.

680 **Figure 6.** **(a)** Non-metric multidimensional scaling plot (NMDS) of the methanogenic  
681 community structures in manure batch reactors based on mcrA sequencing. **(b)** Relative  
682 abundances of methanogens from manure batch reactors incubated at 23 °C and 38 °C.  
683 TA:NaF= tannic acid:sodium fluoride, LS = lignosulfonic acid (10 g/L). The taxonomic  
684 level in **(a)** and **(b)** is denoted with (s) for species level, (g) for genus level, (f) for  
685 family level, (o) for order level, and (c) for class level.

686

687 **Table 1.** Chemical analysis of maize silage digestate batch reactors. VS=volatile solids,  
 688 TS=total solids, TAN=total ammonia nitrogen, Ac=acetic acid, VFA=volatile fatty  
 689 acids.

	VS (%)	TS (%)	TAN (g/L)	pH	Acetic acid (mg/L)	VFA (mg/L)	VS (%)	TS (%)	TAN (g/L)	pH	Acetic acid (mg/L)	VFA (mg/L)
<b>Batch 1</b>				Day 0	Day 30							
Inoc	3.5±0.01	4.8±0.01	1.2±0.2	7.70±0.04	26.7±0.4	26.7±0.4	3.0±0.2	4.2±0.3	1.3±0.1	7.53±0.03	13.8±0.2	26.4±4.1
Inoc+sub			1.0±0.7	7.61±0.03	19.2±2.3	19.2±2.3	3.1±0.2	4.3±0.2	1.4±0.2	7.47±0.01	8.5±7.4	12.2±13.8
Inoc+sub+urea			1.1±0.3	7.65±0.09	21.5±1.7	21.5±1.7	2.9±0.1	4.1±0.1	3.8±0.1	7.92±0.06	327.4±91.6	481±254
Inoc+sub+urea			1.3±0.2	7.00±0.01	22.7±1.6	22.7±1.6	3.9±0.2	4.9±0.3	4.8±0.4	7.31±0.02	4247±238	4494±266
+TA:NaF (10:1 mM)												
Inoc+sub+urea			1.1±0.2	7.66±0.01	401.5±28.4	679.8±42	3.4±0.1	4.9±0.1	4.3±0.1	7.82±0.04	140.0±47.2	170.3±51.9
+LS (10 g/L)						0						
<b>Batch 2</b>				Day0	Day30							
Inoc	3.8±0.02	5.5±0.01	1.5±0.02	7.70±0.01	22.1±1.5	22.1±1.5	3.3±0.2	4.8±0.3	1.2±0.1	7.65±0.01	17.1±1.9	36.2±2.4
Inoc+sub				7.71±0.02	21.8±1.4	25.3±7.4	3.4±0.1	4.9±0.1	1.1±0.2	7.53±0.03	17.5±1.0	35.7±1.8
Inoc+LS (10 g/L)				7.74±0.01	188.3±96.5	319±176	4.5±1.1	6.5±1.3	1.3±0.1	7.62±0.05	28.9±2.0	59.5±2.9
Inoc+				7.40±0.06	23.6±5.6	23.7±5.8	3.4±0.1	4.9±0.2	0.9±0.2	7.44±0.02	14.9±2.5	27.1±2.7
TA:NaF (2.5:1 mM)												
Inoc+				7.19±0.06	24.9±0.6	24.9±0.6	3.5±0.02	5.0±0.04	1.3±0.1	7.42±0.01	13.8±1.0	21.2±1.7
TA:NaF (5:1 mM)												

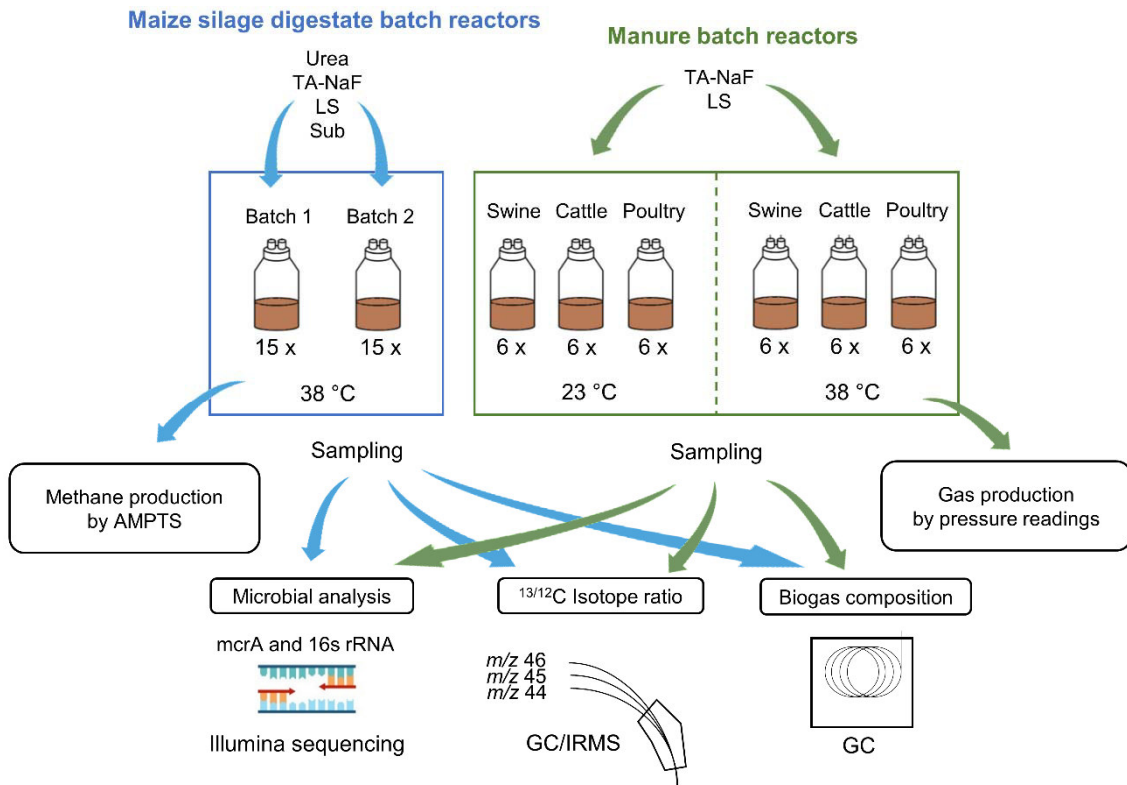
690

691 **Table 2.** Chemical analysis of manure batch reactors. VS=volatile solids, TS=total  
 692 solids, TAN=total ammonia nitrogen, Ac=acetic acid, VFA=volatile fatty acids. Values  
 693 at day 0 are given for the diluted manure.

	VS	TS	TAN	Ac	VFA	VS	TS	TAN	Ac	VFA					
	(%)	(%)	(g/L)	pH	(mg/L)	(%)	(%)	(g/L)	pH	(mg/L)					
<b>Room Temp</b>						<b>Day 0</b>					<b>Day 30</b>				
Poultry litter	2.0±0.2	2.4±0.2	0.4±0.1	7.32	603±26	796±39	1.8	2.2	1.0±0.7	6.1±0.01	4039±45	6301±102			
Poultry litter+5:1 mM TA:NaF							2.7	3.1	0.9±0.2	6.1±0.01	735±125	1152±321			
Poultry litter+LS (10 g/L)							2.0	2.8	0.9±0.2	6.6±0.06	4562±264	6651±317			
Swine	2.0±0.1	3.1±0.1	5.2±0.9	7.68	1078±15	1816±44	2.5	3.9	3.8±0.3	8.1±0.01	44±4	289±2			
Swine+5:1 mM TA:NaF							3.2	4.4	4.1±0.5	7.8±0.04	873±23	1660±131			
Swine+LS (10 g/L)							3.3	5.0	3.4±0.0	8.1±0.03	59±5	305±5			
Cattle	2.0±0.2	2.6±0.2	0.3	1.2±0.2	7.03	1314±320	2157±532	2.8	3.5	0.7±0.2	7.3±0.31	2444±90	3960±133		
Cattle+5:1 mM TA:NaF							3.0	3.7	0.7±0.2	6.0±0.01	4181±102	5552±81			
Cattle+LS (10 g/L)							2.4	3.6	0.7±0.1	7.4±0.62	3460±18	5184±63			
<b>38 °C</b>						<b>Day 0</b>					<b>Day 30</b>				
Poultry litter	2.0±0.2	2.4±0.2	0.4 ± 0.1	7.32	603 ± 26	796 ± 39	1.2	1.5	0.9±0.7	5.9±0.02	3988±788	6738±1276			
Poultry litter+5:1 mM TA:NaF							2.7	3.1	1.1±1.6	5.6±0.12	579±84	833±171			
Poultry litter+LS (10 g/L)							2.0	2.8	1.2±0.0	7.1±0.02	2744±3732	4467±5010			
Swine	2.0±0.1	3.1±0.1	5.2 ± 0.9	7.68	1078 ± 15	1816 ± 44	2.4	3.6	3.4±0.2	8.2±0.04	40±6	264±51			
Swine+5:1 mM TA:NaF							3.1	4.5	3.1±0.2	7.9±0.05	659±794	1358±1245			
Swine+LS (10 g/L)							2.6	4.1	3.8±0.1	8.3±0.05	58±3	316±8			
Cattle	2.0±0.1	2.6±0.2	0.3	1.2 ± 0.2	7.03	1314 ± 320	2157± 532	1.8	2.5	1.0±0.1	7.5±0.34	54±12	127±2		
Cattle+5:1 mM TA:NaF							3.3	4.0	3.2±0.0	7.3±0.01	2325±84	3397±153			
Cattle+LS (10 g/L)							2.1	3.4	1.0±0.1	7.7±0.15	276±34	726±27			

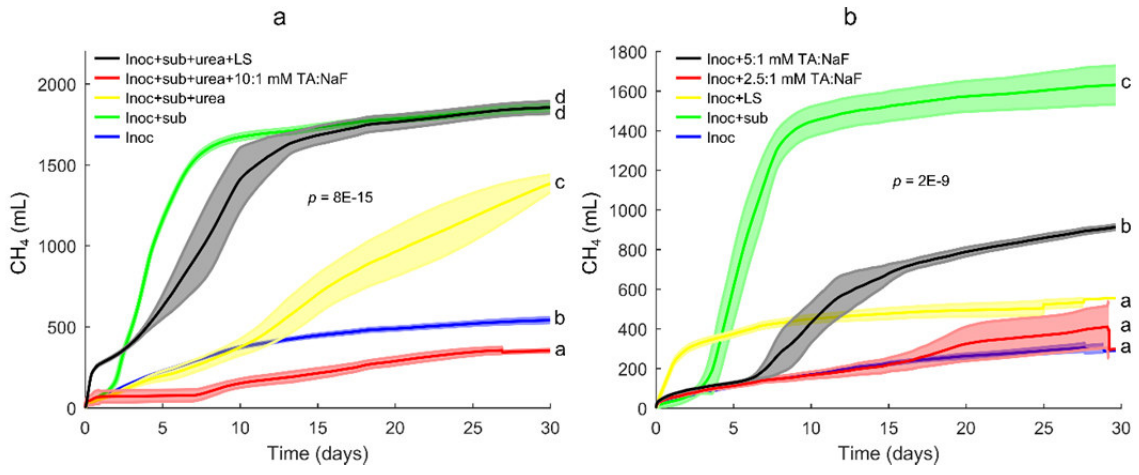
694

695 **Figure 1.**



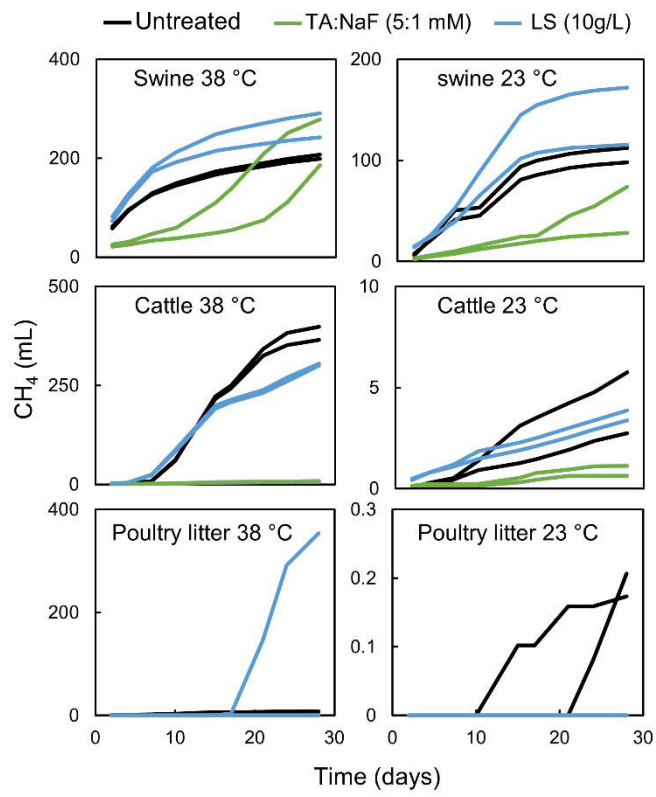
696

697 **Figure 2.**



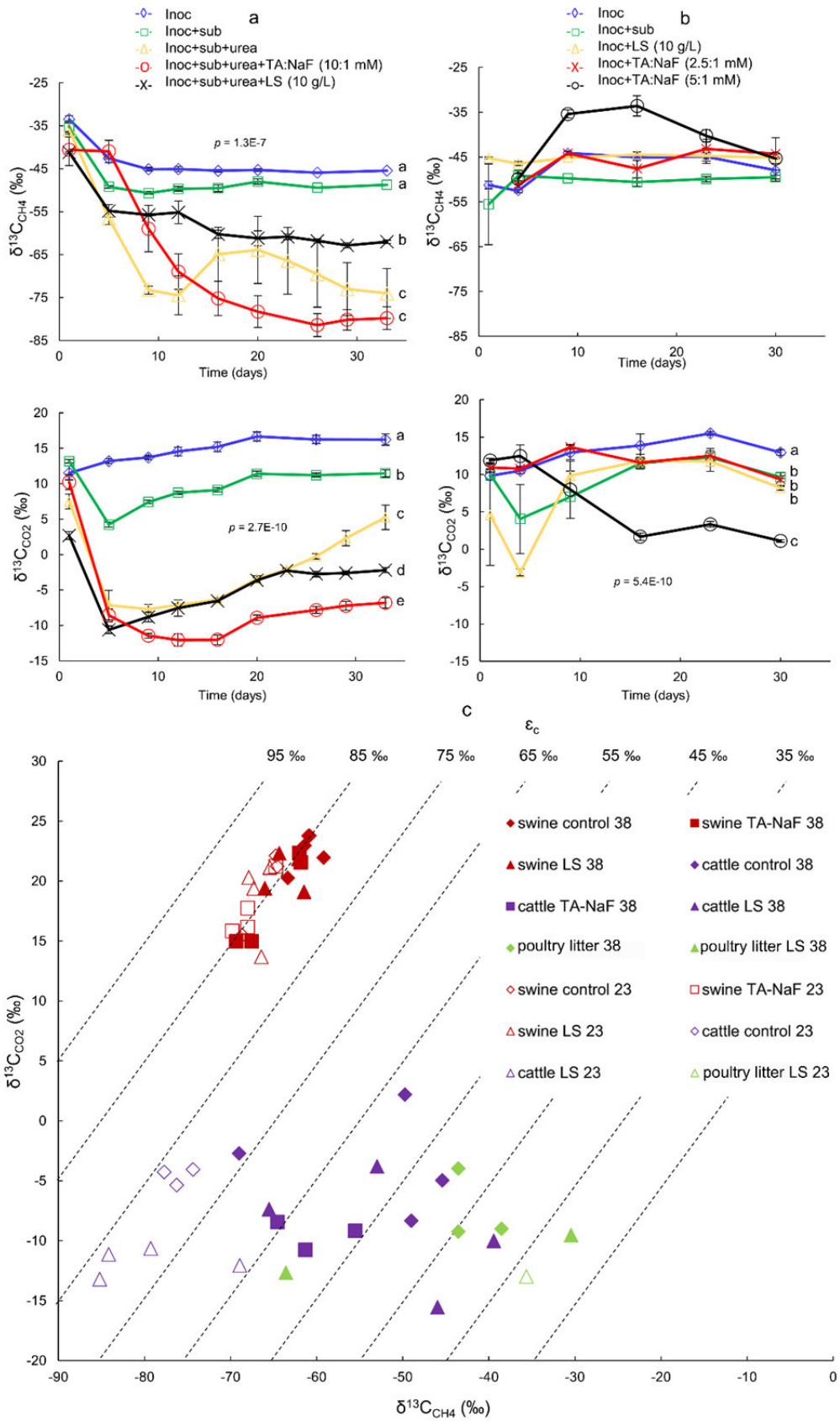
698

699 **Figure 3.**



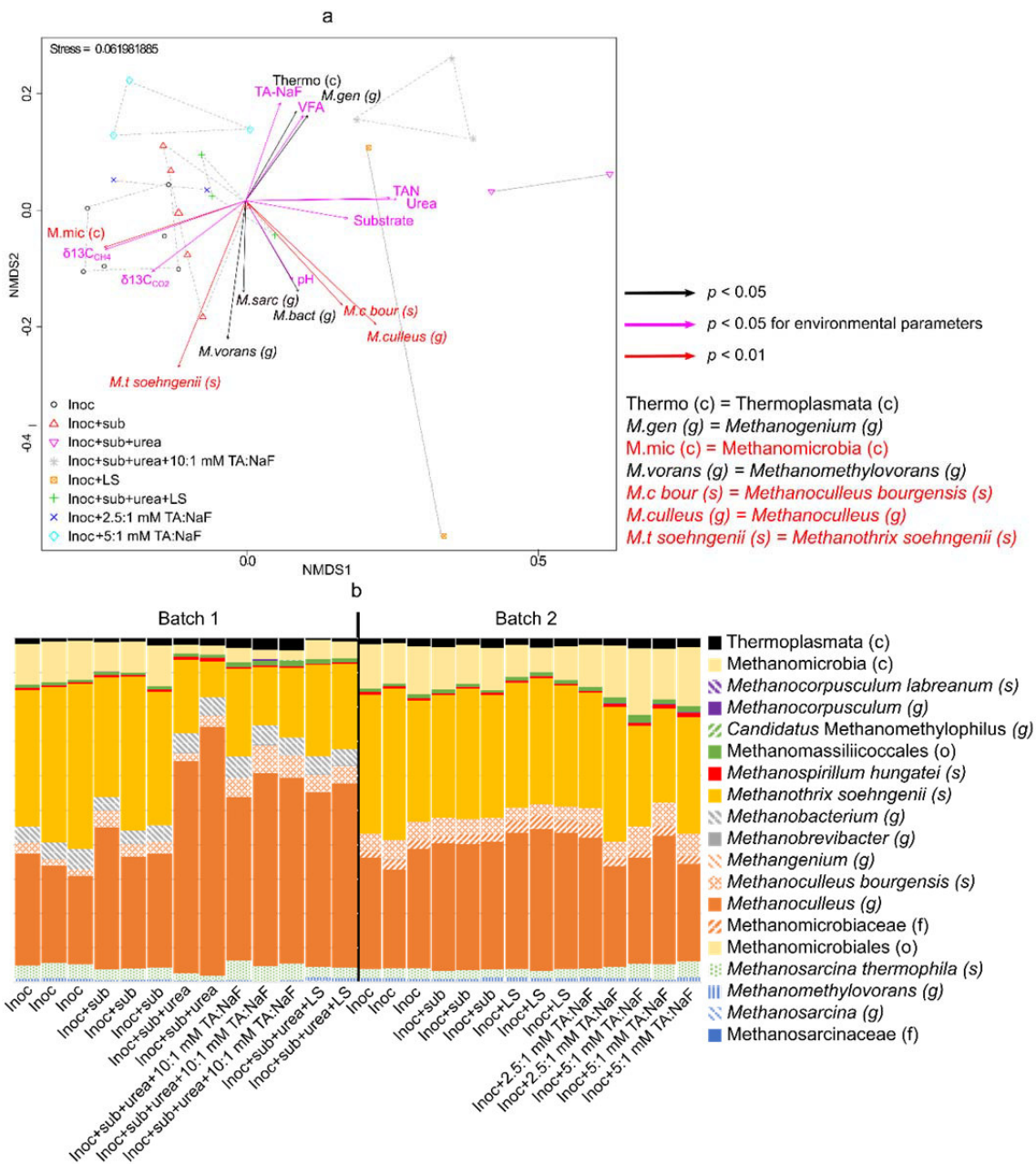
700

701 **Figure 4.**

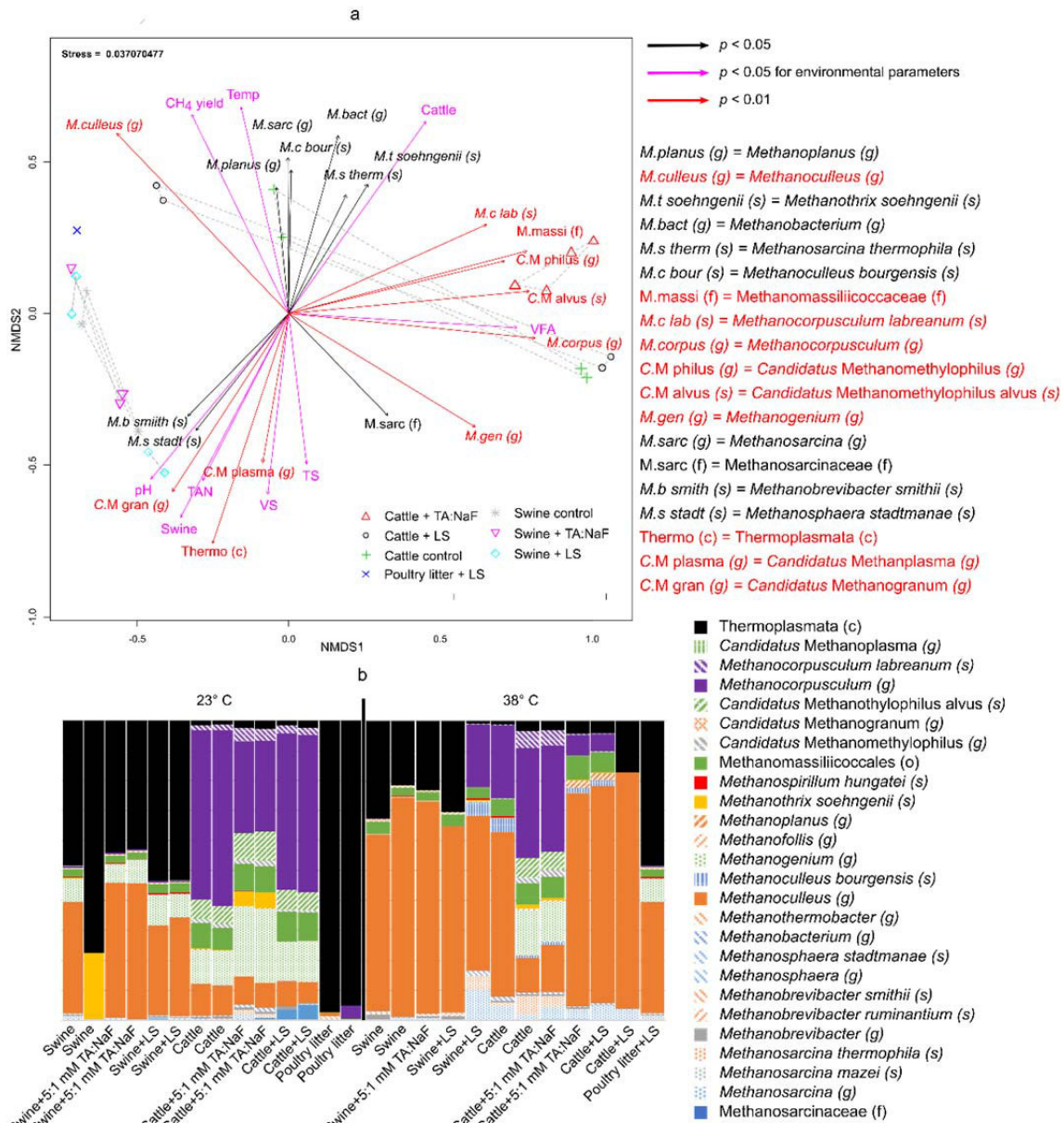


702

703 **Figure 5.**



705 **Figure 6.**



706